Radiation Physics and Chemistry 166 (2020) 108522

Contents lists available at ScienceDirect

Radiation Physics and Chemistry

journal homepage: www.elsevier.com/locate/radphyschem

FT-IR spectral features of DNA as markers for the detection of liver preservation using irradiation

Amany M. Hamad[a], Heba M. Fahmy[a,*], Wael M. Elshemey[a,b]

[a] Biophysics Department, Faculty of Science, Cairo University, Giza, 12613, Egypt
[b] Department of Physics, Faculty of Science, Islamic University, Madinah, Saudi Arabia

ARTICLE INFO

Keywords:
FT-IR spectroscopy
Calf liver
DNA damage
Sterilization
Irradiated food
Gamma irradiation

ABSTRACT

Food preservation, inhibition of foodborne-pathogenic microorganisms, as well as prolonging the shelf life of food products are all achieved through the application of irradiation technology in food preservation. In terms of food safety and for strengthening worldwide trade of irradiated foods, the presence of a trustworthy method for identification of irradiated foodstuff is currently the focus of attention. Since DNA has a documented high sensitivity to ionizing radiation, this work introduces a method for the detection of gamma-irradiated (3 kGy) calf liver through measurements of Fourier-transform infrared (FT-IR) spectra of their extracted DNA. Results show characteristic FT-IR bands that yield significant differences between irradiated and control calf liver samples. The guanine nucleoside band at 1491 cm^{-1} provides the most significant characterization.

1. Introduction

Improving food safety (meat and meat products, fish, grains, and fruits, etc.) by getting rid of foodborne pathogens is considered as one of the quarantine interests and purposes. Food irradiation is an effective technology accepted for controlling foodborne-pathogens and accordingly, prolongs, as long as possible, food product shelf life (WHO, 1999; Joshi et al., 2018, Kyung et al., 2019). Definite pathogens causing meat and meat product contamination (*Escherichia coli* O157:H7, *Salmonella enterica* serovar Enteritidis, *Campylobacter jejuni*, and *Yersinia enterocolitica*) can be inactivated by irradiation at doses of 2–7 kGy (Farkas, 2006; Henriques et al., 2014). In other words, food decontamination, while preserving the nutritional value of food, can be achieved at low doses ($^{<}$10 kGy) of gamma-irradiation (https://onlinelibrary.wiley.com/action/doSearch?ContribAuthorStored=THAYER%2C+DW, Thayer et al., 1995; de Souza et al., 2019). In particular, fresh and frozen red meats have received authorization for irradiation with doses up to 4.5 and 7.0 kGy, respectively (Li et al., 2015; Roberts, 2016).

Based on the reported importance of food irradiation technology and to ensure good international trading, health and safety of consumer, there is always a need for an easy, fast, sensitive and inexpensive means for the discrimination between irradiated and non-irradiated foodstuffs. There are currently 10 authorized standard methods for the detection of irradiated foods that are used in Europe as general Codex methods (Delincée, 2002; Zanardi et al., 2018).

Since DNA is a main component in all raw foodstuffs of plant and animal origins and since DNA is a vulnerable target for ionizing radiation (IR) so, the identification of irradiated foods can be achieved by following up changes in DNA structure induced by the interaction of radiation (Fukui et al., 2017; Eugster et al., 2018). Contextually, one of the standard methods permitted by the European Committee for Standardization (CEN) for irradiated food detection is DNA comet assay (EN 13784 (2001). Unfortunately, this method is time-consuming besides that comet image analysis is complicated (Miyahara et al., 2000; Verbeek et al. 2008; Cetinkaya et al., 2016).

On the other hand, vibrational spectroscopic techniques (Fourier transform infrared, FT-IR, and Raman) have proved their potential to provide information on the structural changes of biomolecules such as DNA of any size (Native DNA, short oligonucleotides, etc.). These powerful techniques received increased attention in the biophysical and biomedical research fields (Kneipp et al., 2010; Muntean et al., 2013; Stefan et al., 2014; Anastassopoulou et al., 2019). Interestingly, no labeling (such as labeling stains or isotopes) is needed in the methodology of these spectroscopic techniques. In particular, many studies demonstrated the capability of FT-IR spectroscopy to detect DNA damage (Dovbeshko et al., 2000; Stefan et al., 2014; Ovissipour et al., 2019) where functional chemical groups can be assigned by specific spectral vibration bands. Furthermore, the vibrational and rotational motions of the DNA molecule can be changed in response to the formation of

* Corresponding author.
E-mail addresses: heba_moh_fahmi@yahoo.com, hfahmy@sci.cu.edu.eg (H.M. Fahmy).

https://doi.org/10.1016/j.radphyschem.2019.108522
Received 25 June 2019; Received in revised form 1 October 2019; Accepted 8 October 2019
Available online 09 October 2019
0969-806X/

mutagenic derivatives as a result of the DNA bases oxidation (Cooke et al., 2003). In a study directed by Le-Tien et al. (2007), the structural changes of DNA isolated from *pantoea agglomerans* bacterium have been examined by FT-IR spectroscopy following the inactivation of this bacterium by different doses of gamma irradiation. Additionally, FT-IR can be applied to detect subtle disruptions in DNA structure exhibited by drug interactions (Malins et al., 2002; Kanakis et al., 2005), temperature (Lee et al., 2004) and counter ions (Hackl et al., 2005).

The objective of the present study is, therefore, to investigate the feasibility FT-IR DNA spectroscopy as a new method for the detection of irradiated calf liver (a foodstuff of animal origin that is preserved by irradiation).

2. Materials and methods

2.1. Materials

Fresh calf liver was purchased from a local slaughterhouse. The following chemicals were used for the extraction of DNA: sodium chloride (NaCl), homogenizing buffer (50 mM Tris-HCl, pH 8.0; 25 mM EDTA and 0.4 M NaCl), sodium dodecyl sulfate (SDS), proteinase K, and 100% ethanol. All chemicals were from the analytical grade that are commercially available. The irradiation source was cobalt-60 (Indian Gamma Cell, 60Co) located at the Egyptian Atomic Energy Authority (EAEA), Naser City, Cairo, Egypt.

2.2. Methods

2.2.1. Sample preparation

Liver slices from the purchased calf liver (3 slices for each of the tested dose and control) were prepared and each slice was packaged separately in polyethylene bags. Thereafter, all slices were preserved overnight in a freezer at −20 °C until irradiated.

2.2.2. Calf liver irradiation

On the next day, gamma-radiation from cobalt-60 (^{60}Co) (Indian Gamma Cell, ^{60}Co) was used as an irradiation source for frozen liver samples. The applied dose was 3 kGy with a dose rate of 1.185 kGy/h. Crushed ice-polyethylene bags were placed surrounding liver slices during irradiation period to avoid any possible change in the taste or nutritional value of liver samples. After irradiation, the irradiated liver slices were re-preserved in the freezer.

2.2.3. Extraction and purification of calf liver DNA

The extraction protocol of calf liver DNA from each liver slice was performed according to the procedures reported by Biase et al. (2002) with minor modifications. Briefly, the 2nd day following irradiation, in the presence of 800 μL sterile salt ice-cold homogenizing buffer (50 mM Tris-HCl, pH 8.0; 25 mM EDTA and 0.4 M NaCl) and using Glass Dounce Tissue Grinder Homogenizer Cell Mortar with Pestle, 0.4 mg was taken from each frozen calf liver slice (the non-irradiated control and the 3 kGy irradiated test samples) and homogenized. The homogenized tissues were transferred into sterile falcon tubes and incubated at 65 °C for 90 min after being mixed with 0.69 M SDS and 0.69 mM proteinase K. For the precipitation of proteins and cellular debris, 700 μL of 6 M saturated-NaCl was added to each tube then vortexed for 30 s. Thereafter, samples were incubated at 4 °C for 20 min and centrifuged (20 min, 12,000 rpm) at room temperature. After centrifugation, the supernatant was transferred to a fresh sterile tube and an equal volume of cold 100% ethanol was added to each tube. Each sample tube was kept at −20 °C for 1 h for complete precipitation of DNA and then was subject to centrifugation (25 min, 12,000 rpm) at 4 °C. Finally, all DNA pellets were washed once using 100% ethanol and twice suing 70% ethanol. DNA pellets were then allowed to dry in air.

2.2.4. Acquisition of DNA FT-IR spectra

High quality DNA spectra with no interference from water bands can be obtained by selecting dried DNA samples for FT-IR spectral acquisition (Le-Tien et al., 2007, Han et al., 2018). All FT-IR spectral acquisitions of dried DNA pellets were performed in the absorption mode using Bruker FTIR-Alpha 1 spectrophotometer. Complete grindig of 100 mg of anhydrous potassium bromide (KBr) with 1 mg of each dried DNA pellet was carried out to achieve almost transparent and compressed tablets (around 13 mm diameter and 1 m thick) as the finalized form for the acquisition of FTIR spectra. The tablets were scanned in an inert atmosphere. The acquisition of spectra with a total of 64 co-added scans was carried out for each sample in the wavenumber range 4000–400 cm^{-1} at a spectral resolution of 4 cm^{-1}. The resultant spectra underwent to baseline corrections prior to any spectral analysis for the removal of background signals.

2.2.5. Pre-processing and analysis of FTIR spectra

Acquired FT-IR spectra (4000-400 cm^{-1}) were peak-normalized at 1011.51 cm^{-1} (the maximum intensity (I) in the DNA range, 1800-800 cm^{-1}). The peak at 1011.51 cm^{-1} is due to the vibration modes of DNA sugar (Letellier et al., 1989; Liquier and Taillandier, 1996). The average FTIR spectra were then calculated for DNA from both control and 3 kGy-gamma irradiated calf liver samples.

All comparisons between control and irradiated samples were carried out using bands in the spectral region of DNA (1800–800) cm^{-1} (Kondepati et al., 2006; Muntean et al., 2014; Han et al., 2019).

The peak position (PP), peak intensity (I) as well as the area under the peak (AUP) were derived as characterization parameters from each spectrum. For each selected peak, the value of the area under the peak was calculated depending on the method of trapezoidal integration with the aid of Microsoft Excel (2010).

A difference spectrum (average infrared spectrum of DNA from 3 kGy irradiated liver samples - average infrared spectrum of DNA from non-irradiated control liver samples) was calculated to clearly validate the possible alteration in the intensity of each peak. According to the following equation, the percentage change in both intensity and AUP was determined from DNA spectrum of irradiated-livers.

$$Percentage\ \ change = (irradiated - control)/control \quad x \quad 100 \qquad (1)$$

Furthermore, for the precise evaluation of the shifts in the PP, the FT-IR second derivative spectra in the DNA spectral region, 1800-800 cm^{-1} were calculated after 7-point Savitzky–Golay smoothing using OriginPro 8 software (Kondepati et al., 2006; https://scholar.google.com.eg/citations?user=gZ5evfQAAAAJ&hl=en&oi=sra, Elshemey et al., 2016).

2.2.6. Statistical analysis

Measurements were carried out on triplicate control and irradiated samples. Results are presented as mean ± standard deviation. The significance ($p < 0.05$) of data was calculated using the Student's t-test with the aid of the Statistical Package for the Social Sciences (SPSS) version 19.

3. Results and discussion

The purity of DNA samples was evaluated spectrophotometrically by determining the A260/A280 and A260/A230 ratios and were found to be 1.86 ± 0.09 and 1.76 ± 0.12 as average values, respectively. With respect to the A260/A280 ratio, the values were satisfactory indicating that the isolated DNA contained no protein contamination (Glasel, 1995; Agarwal et al., 2013). Although RNase was not used, we have relied on that the purity ratios for all extracted DNA samples were comparable.

The molecular structure of DNA from control liver samples and the changes exhibited in response to the irradiation of liver by gamma irradiation in irradiated samples are presented in the average FT-IR

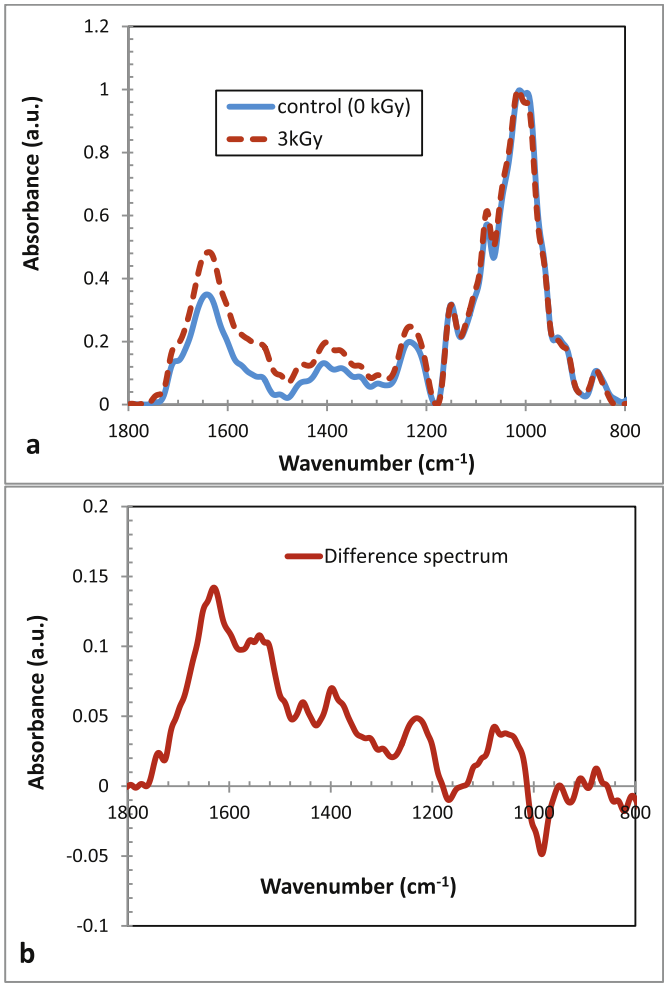

Fig. 1. a) Average FT-IR absorption spectra (1800-800 cm^{-1}) of DNA samples from non-irradiated control (light blue) and 3 kGy-irradiated livers (dotted red), after peak normalization of three individual spectra per sample. b) FT-IR difference spectrum (average infrared spectrum of DNA from 3 kGy irradiated liver samples - average infrared spectrum of DNA from non-irradiated control liver samples). (For interpretation of the references to colour in this figure legend, the reader is referred to the Web version of this article.)

spectra in the 1800-800 cm^{-1} range as depicted in Fig. 1a. The differences in peak intensities between control and irradiated samples are represented in the FT-IR difference spectrum (Fig. 1b). The difference spectrum (Fig. 1b) shows many positive peaks which reflect the elevation in intensities of DNA functional groups compared to irradiated liver samples.

The percentage change in the intensity, PP and AUP parameters of the selected bands are described in details in Table 1. The shift in wavenumber of all bands is represented using the second derivative spectra, as demonstrated in Fig. 2 and as tabulated in Table 1. The assignments of examined peaks are based on the information reported in the literature (Taillandier and Liquier, 1992; Banyay et al., 2003; Socrates, 2004; Adali et al., 2013; Tripon et al., 2016) and are also shown in Table 1.

Generally, the FT-IR spectrum of DNA contains 3 main regions which are; the region of the sugar-phosphate DNA backbone (1250–900) cm^{-1}, base-sugar region (1500–1250) cm^{-1} and DNA base region (1800–1500) cm^{-1} (Taillandier and Liquier, 1992; Lindqvist and Gräslund, 2001; Gomes et al., 2009; Muntean et al., 2013). In the wavenumber region 1200-800 cm^{-1}, DNA extracted from irradiated livers exhibited no significant alterations in the absorption modes regarding wavenumber shift, intensity and AUP, as compared with the DNA from non-irradiated control liver samples. However, there are still noticeable differences to be detected, particularly in the spectral region from 1200 to 1722 cm^{-1}. An analysis of this region will be described in the following sections.

3.1. The region of DNA backbone (800–1250) cm^{-1}

FTIR spectra of control and irradiated samples (Fig. 1a) and their corresponding difference spectrum (Fig. 1b) show that there is only one peak in this region that exhibits significant changes between DNA extracted from control and gamma-irradiated liver samples. This peak belongs to O–P–O anti-symmetric ($\nu_{asym}\ PO_2^-$) stretching vibration in A-form DNA (Taillandier and Liquier, 2002), positioned at 1242.24 cm^{-1} and after irradiation, this peak showed no change in position as detected from the 2nd derivative spectra (Fig. 2). On the other hand, its intensity and AUP parameters of irradiated samples increased significantly ($p^< 0.05$) by 21.05% and 27.05%, respectively, with respect to those of the control group.

The present results are in line with the results reported by Lipiec et al. (2012) who found that by using the FTIR microspectroscopy, the area corresponding to O–P–O backbone peak increased with increasing proton irradiation dose for single PC-3 cells (prostate cancer cell line). They explained that this increase in the area under this DNA backbone peak was due to emerging gross free phosphate molecules and/or presence of DNA strand breaks. Moreover, the increase in band intensity of this peak matches what has been reported by Muntean et al. (2014), in response to irradiation of DNA extracted from *E. coli* B by ultraviolet (UV) radiation.

3.2. The region of base-sugar (1500–1250) cm^{-1}

As an overview, the vibration bands in this region of DNA spectra from irradiated samples exhibit a significant increase in both intensity and AUP in comparison to those from control samples (Table 1), these include:

1 Deoxycytidine (dC) vibrations (N3 = C4, C4–C5, N1–C2, C2–N3, N1–C6 and C5 = C6) at approximately 1298.89 cm^{-1}.
2 Vibrations due to C2′-endo/anti of deoxythymidine (dT) at approximately 1332.88 cm^{-1}.
3 Vibrations due to sugars: C2′/C3′-endo of deoxyguanosine (dG) and deoxyadenosine (dA) nucleosides around 1369.96 cm^{-1}.
4 Vibrations assigned to deoxyribose: C3′-endo for residues of all bases (A-form conformation) at approximately 1409.11 cm^{-1}.
5 Deoxyadenosine (dA) vibrations of N1 = C6–N6 in either A- or B-form around 1454.43 cm^{-1}.
6 Vibrations at approximately 1494.6 cm^{-1} associated with N7 = C8, C8–N9, C4 = C5, C4–C9 and N–C8–H of deoxyguanosine (dG), (Letellier et al., 1989).

As noted from the 2nd derivative spectra, the three vibration modes 1494.6 cm^{-1}, 1409.11 cm^{-1}, and 1369.96 cm^{-1} significantly exhibit a shift in PP (Fig. 2 and Table 1) of irradiated samples compared to control. From the results of aforementioned peaks, it can be noticed that the vibration mode of dG at 1494.6 cm^{-1} seems to exhibit the maximum increase in both intensity and AUP by 200% and 176.92%, respectively.

3.3. The region of DNA nucleobases (1800-1500 cm^{-1})

In this region, the stretching vibrations belonging to cytosine (C) ring are represented at an average wavenumber of 1528.59 cm^{-1} (Table 1) for control samples. In the case of irradiated liver samples, this band shifts significantly ($p^< 0.05$) to a lower wavenumber (1524.47 cm^{-1}). It has been previously reported that the loss of hydrogen bonding between base pairs lead to downward shifting of the

Table 1
Detailed comparative analysis between control and irradiated calf liver samples at thirteen selected infrared absorbance bands in the region (1800-800 cm^{-1}) with tentative assignments (Taillandier and Liquier, 1992, 2002; Banyay et al., 2003; Tripon et al., 2016). The comparison parameters are the peak position (PP), intensity (I), area under peak (AUP), percentage intensity (%I) and percentage area under peak (%AUP). Data are represented as mean ± standard deviation. The symbol "a" denotes significant ($p < 0.05$) variation from control.

		3 kGy			Control				
%AUP	%I	AUP	I	PP(cm^{-1})	AUP	I	PP (cm^{-})	Tentative assignment	
27.05	21.05	14.89 ± 0.03 [a]	0.23 ± 0.00 [a]	1242.24	11.72 ± 0.89	0.19 ± 0.01	1242.24	**ν_{asym} PO_2^-, probable A-form**	**DNA backbone region**
40.88	28.57	2.55 ± 0.00 [a]	0.09 ± 0.00 [a]	1297.86	1.81 ± 0.00	0.07 ± 0.00	1298.89 ± 1.03	**(N3 = C4, C4–C5, N1–C2, C2–N3, N1–C6 and C5 = C6) vib. in dC**	**Base-sugar region**
42.19	36.36	3.37 ± 0.02 [a]	0.12 ± 0.00 [a]	1331.85 ± 1.03	2.37 ± 0.04	0.088 ± 0.00	1332.88	**(C2′-endo/anti) in dT**	
47.82	41.67	7.14 ± 0.00 [a]	0.17 ± 0.00 [a]	1376.14 [a]	4.83 ± 0.19	0.12 ± 0.0	1369.96 ± 2.06	**(C2′-endo/anti) in dA and dG**	
49.21	53.85	6.64 ± 0.06 [a]	0.2 ± 0.00 [a]	1401.9 ± 1.03 [a]	4.45 ± 0.10	0.13 ± 0.00	1409.11 ± 2.06	**(C3′-endo) residues of all bases (A-form)**	
87.95	85.71	4.68 ± 0.10 [a]	0.13 ± 0.00 [a]	1454.43	2.49 ± 0.26	0.07 ± 0.01	1454.43 ± 2.06	**(N1 = C6–N6) in dA A-/B-forms**	
176.92	200	2.16 ± 0.07 [a]	0.09 ± 0.01 [a]	1491.54 [a]	0.78 ± 0.25	0.03 ± 0.01	1494.6 ± 1.03	**(N7 = C8, C8–N9, C4 = C5, C4–C9, N–C8–H) in dG**	
123.88	100	10.50 ± 0.65 [a]	0.18 ± 0.01 [a]	1524.47 [a]	4.69 ± 0.37	0.09 ± 0.01	1528.59	**In-plane vib of C**	**DNA bases region**
63.49	83.33	4.12 ± 0.25 [a]	0.22 ± 0.01 [a]	1572.88 ± 1.46	2.52 ± 0.3	0.12 ± 0.02	1571.85	**N–H**	
55.60	55	7.64 ± 0.38 [a]	0.31 ± 0.01 [a]	1598.63 [a]	4.91 ± 0.44	0.20 ± 0.02	1600.69	**H–N–H**	
41.40	42.42	19.57 ± 0.80 [a]	0.47 ± 0.02 [a]	1629.54	13.84 ± 0.46	0.33 ± 0.01	1630.57 ± 1.03	**(C=N; C=C) ring vib in A**	
43.05	31.43	38.38 ± 2.03 [a]	0.46 ± 0.02 [a]	1651.17 ± 1.03 [a]	26.83 ± 1.72	0.35 ± 0.01	1644.99 ± 3.09	**Essentially str. vib. of (C4 = O4) in T**	
33.92	23.08	2.29 ± 0.07 [a]	0.16 ± 0.01 [a]	1712.97 ± 1.46	1.71 ± 0.38	0.13 ± 0.03	1711.94	**(C6 = O6) str. vib of G**	

Abbreviations: v: wavenumber, str: stretching, asym: asymmetric, vib: vibration, dC: deoxycytidine, dT: deoxythymidine, dG: deoxyguanosine, dA: deoxyadenosine, C: cytosine, A: adenine, T: thymine, and G: guanine.

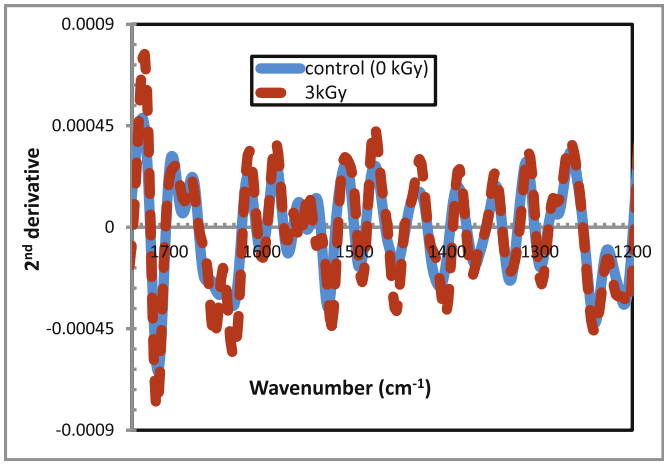

Fig. 2. FT-IR second-derivative spectra of DNA samples from non-irradiated control (light blue) and 3 kGy-irradited livers (dotted red) in the region 1760-1200 cm^{-1}. (For interpretation of the references to colour in this figure legend, the reader is referred to the Web version of this article.)

cytosine band as a result of un-stacking of DNA bases (Dong et al., 2004). Furthermore, this band in DNA from irradiated liver samples exhibits marked significant ($p^{<}$ 0.05) increases in both intensity (by 100%) and AUP (by 123.88%) parameters with respect to control.

Based on the 2nd derivative spectra (Fig. 2), there are two obvious vibrations at 1571.85 cm^{-1} and 1600.69 cm^{-1}, related mainly to N–H bending and NH_2 scissoring, respectively. For DNA from irradiated liver samples, the vibration of N–H bond displays significant ($p^{<}$ 0.05) increase by 83.33% and 63.49% of intensity and AUP parameters (Table 1). With regard to NH_2 scissoring band (1600.69 cm^{-1}) in the DNA spectrum of irradiated liver samples, the intensity and AUP parameters also exhibit significant ($p^{<}$ 0.05) increase (55% and 55.60%, respectively) with respect to control. However, this band show statistically considerable ($p = 0.05$) shift to lower wavenumber (1598.63 cm^{-1}) in irradiated samples compared to control. This rise in intensities of these two bands agrees with that reported in the study of Le-Tien et al. (2007), in their effort for the inactivation of *Pantoea agglomerans* bacteria using ^{60}Co-gamma irradiation. They suggested that nucleobase rings with unconnected NH_2 and N–H groups might result in the increase in the intensity of both bands.

From the 2nd derivative spectra of control and irradiated samples a band can be clearly observed at~ 1630.57 cm^{-1}. This band contains contributions from the ring of adenine (A) base. For irradiated samples, the mean values of intensity and AUP increase significantly ($p^{<}$ 0.05) by 42.42% and 41.40, respectively compared to control.

Additionally, a band that is characterized by a high intensity can be seen at 1644.99 ± 3.09 cm^{-1} in control liver samples. This band is significantly ($p^{<}$ 0.05) shifted to a higher wavenumber (1651.17 ± 1.03 cm^{-1}) in irradiated samples. This band corresponds mainly to the stretching vibrations of C4 = O4 of thymine (T) (Liquier and Taillandier, 1996) but there are minor involvements from C6 = O6, C=N and C = C guanine (G) stretching vibrations as well (Zhou-Sun et al., 1997). This band also reveals a significant ($p^{<}$ 0.05) increase in both intensity (by 31.43%) and AUP (43.05%) in the irradiated sample compared to control. Le-Tien et al. (2007) reported comparable increase in peak intensity after exposure of their bacterium to gamma irradiation of doses higher than ≥5 kGy and concluded that modifications of the chemical structure and composition of DNA bases rings might be the reason of this subsequent increase in band intensity.

The in-plane stretching vibration of carbonyl group at guanine (G) base ring (C6 = O6) positioned at 1711.94 cm^{-1} (Banyay et al. 2003) also show significant ($p^{<}$0.05) increase in both intensity (by 23.08%) and AUP (by 33.92%) in the spectrum from irradiated liver samples.

This rise in intensities of irradiated samples in the region of DNA nucleobases (1800-1500 cm^{-1}) can be attributed to the destabilization of the DNA helix (Jangir et al., 2010). Furthermore, the increase in intensities are similar to those described by Zhang et al. (2012). Stacking defect of the nitrogenous bases is a conclusive explanation provided by authors who tested the damage of calf thymus DNA through the interaction with triadimenol as a commonly used pesticide against fungi infecting vegetarian foods. It is noteworthy that the peak at 1494 cm^{-1}, referring to guanine nucleoside (dG), exhibited the most prominent variation from control.

Collectively, the results presented here are consistent with the fact

that the attacking reactive oxygen species (ROS), in particular hydroxyl radicals (·OH), on DNA helix can evoke a number of reactions thus resulting in modifications of the deoxyribose sugar and nucleobases (Beckman and Ames, 1997; Lee et al., 2009; Nikitaki et al., 2015). These oxidative modifications appear in the form of changes in the vibrational modes of the DNA molecule groups as detected by FT-IR. ROS specifically target guanine (G) base (Pouget et al., 2002) and this in harmony with the drastic changes in guanine related peaks.

To sum up, it has been shown that the FT-IR spectra of DNA extracted from irradiated calf liver (at 3 kGy, a dose that is used for liver preservation) contain plenty of characteristic features that can successfully detect such irradiation. This is an extremely important result as it supports the consumer right to know whether or not the liver he/she is eating has been preserved by irradiation. Based on the discussed results, one can select the following intensity and AUP parameters, in order, as the most outstanding parameters for such purpose: dG nucleoside at about 1494.6 cm^{-1}, C base at 1528.59 cm^{-1} and dA nucleoside at 1454.43 cm^{-1}. It is noteworthy that all of the investigated intensity and AUP parameters provide significant differences between irradiated and control samples. Moreover, a number of significant shifts in PP are also indicative of such differences, yet to a lower extent.

4. Conclusion

From the present work, it was shown that FT-IR spectral analysis could reveal information on the changes occurring in DNA of irradiated calf liver for the purpose of food preservation as an animal-based foodstuff. Considering the feasibility of the technique, FTIR is a simple and rapid technique (few seconds for obtaining a spectrum). It is sensitive and requires no labeling (such as labeling stains or isotopes). Moreover, the analysis of FTIR can be carried using any available statistical software. Based on the present findings, it could be suggested that the most prominent peaks for such purpose are dG nucleoside at about 1494.6 cm^{-1}, C base at 1528.59 cm^{-1} and dA nucleoside at 1454.43 cm^{-1}. They could be used as a useful biomarker for the detection of liver preserved by irradiation. The present work could be further generalized by performing studies to investigate the possibility to apply the same DNA-FT-IR method to detect other irradiated foodstuff at different doses.

Declaration of competing interest

The authors declare no conflict of interest.

References

Adali, T., Bentaleb, A., Elmarzugi, N., Hamza, A.M., 2013. PEG–calf thymus DNA interactions: conformational, morphological and spectroscopic thermal studies. J. Biol. Macromol. 61, 373–378. https://doi.org/10.1016/j.ijbiomac.2013.07.024.

Agarwal, S., Jangir, D.K., Mehrotra, R., 2013. Spectroscopic studies of the effects of anticancer drug mitoxantrone interaction with calf-thymus DNA. J. Photochem. Photobiol., B 120, 177–182. https://www.ncbi.nlm.nih.gov/pubmed/23266050.

Anastassopoulou, J., Kyriakidou, M., Malesiou, E., Rallis, M., Theophanides, T., 2019. Infrared and Raman spectroscopic studies of molecular disorders in skin cancer. In Vivo 33 (2), 567–572. https://doi.org/10.21873/invivo.11512.

Banyay, M., Sarkar, M., Gräslund, A., 2003. A library of IR bands of nucleic acids in solution. Biophys. Chem. 104 (2), 477–488. https://doi.org/10.1016/S0301-4622(03)00035-8.

Beckman, K.B., Ames, B.N., 1997. Oxidative decay of DNA. J. Biol. Chem. 272 (32), 19633–19636. https://doi.org/10.1074/jbc.272.32.19633.

Biase, F.H., Franco, M.M., Goulart, L.R., Antunes, R.C., 2002. Protocol for extraction of genomic DNA from swine solid tissues. Genet. Mol. Biol. 25 (3), 313–315. https://doi.org/10.1590/S1415-47572002000300011.

Cetinkaya, N., Ercin, D., Özvatan, S., Erel, Y., 2016. Quantification of applied dose in irradiated citrus fruits by DNA Comet Assay together with image analysis. Food Chem. 192, 370–373. https://doi.org/10.1016/j.foodchem.2015.07.027.

Cooke, M.S., Evans, M.D., Dizdaroglu, M., Lunec, J., 2003. Oxidative DNA damage: mechanisms, mutation, and disease. FASEB J. 17 (10), 1195–1214. https://doi.org/10.1096/fj.02-0752rev.

Delincée, H., 2002. Analytical methods to identify irradiated food—a review. Radiat. Phys. Chem. 63 (3–6), 455–458. https://doi.org/10.1016/S0969-806X(01)00539-4.

de Souza, H.B., da Costa Henry, F., Martins, M.L.L., Quirino, C.R., Júnior, J.D.A.M., Júnior, A.C.S., de Oliveira, T.C., de Jesus, E.F.O., 2019. Irradiation of reduced-sodium uncooked lamb sausage: antimicrobial efficacy and physicochemical impact. Braz. J. Microbiol. 50 (1), 231–235. https://doi.org/10.1007/s42770-018-0016-3.

Dong, R., Yan, X., Pang, X., Liu, S., 2004. Temperature-dependent Raman spectra of collagen and DNA. Spectrochim. Acta A Mol. Biomol. Spectrosc. 60 (3), 557–561. https://doi.org/10.1016/S1386-1425(03)00262-2.

Dovbeshko, G.I., Gridina, N.Y., Kruglova, E.B., Pashchuk, O.P., 2000. FTIR spectroscopy studies of nucleic acid damage. Talanta 53 (1), 233–246. https://doi.org/10.1016/S0039-9140(00)00462-8.

Elshemey, W.M., Ismail, A.M., Elbialy, N.S., 2016. Molecular-level characterization of normal, Benign, and Malignant breast tissues using FTIR spectroscopy. J. Med. Biol. Eng. 36 (3), 369–378. https://doi.org/10.1007/s40846-016-0133-0.

EN 13784, 2001. Foodstuffs—DNA Comet Assay for the Detection of Irradiated Foodstuffs—Screening Method. European Committee of Standardization (CEN), Brussels.

Eugster, A., Murmann, P., Känzig, A., Breitenmoser, A., 2018. A specific but nevertheless simple real-time PCR method for the detection of irradiated food shown detailed at the example of garlic (Allium sativum). Eur. Food Res. Technol. 244, 819–825. https://doi.org/10.1007/s00217-017-2998-8.

Farkas, J., 2006. Irradiation for better foods. Trends Food Sci. Technol. 17 (4), 148–152. https://doi.org/10.1016/j.tifs.2005.12.003.

Fukui, N., Takatori, S., Kitagawa, Y., Okihashi, M., Ishikawa, E., Fujiyama, T., Kajimura, K., Furuta, M., Obana, H., 2017. Determination of irradiation histories of raw beef livers using liquid chromatography–tandem mass spectrometry of 5, 6-dihydrothymidine. Food Chem. 216, 186–193. https://doi.org/10.1016/j.foodchem.2016.08.036.

Glasel, J., 1995. Validity of nucleic acid purities monitored by 260 nm/280 nm absorbance ratios. Biotechniques 18 (1), 62–63. https://www.ncbi.nlm.nih.gov/pubmed/7702855.

Gomes, P.J., Ribeiro, P.A., Shaw, D., Mason, N.J., Raposo, M., 2009. UV degradation of deoxyribonucleic acid. Polym. Degrad. Stab. 94 (12), 2134–2141. https://doi.org/10.1016/j.polymdegradstab.2009.09.013.

Hackl, E.V., Kornilova, S.V., Blagoi, Y.P., 2005. DNA structural transitions induced by divalent metal ions in aqueous solutions. Int. J. Biol. Macromol. 35 (3–4), 175–191. https://doi.org/10.1016/j.ijbiomac.2005.01.011.

Henriques, L.S.V., Henry, F.D.C., Barbosa, J.B., Ladeira, S.A., Pereira, S.M.D.F., Antonio, I.M.D.S., Teixeira, G.N., Martins, M.L.L., Vital, H.D.C., Rodrigues, D.D.P., Reis, E.M.F.D., 2014. Elimination of coliforms and Salmonella Spp. In sheep meat by gamma irradiation treatment. Braz. J. Microbiol. 44 (4), 1147–1153. https://doi.org/10.1590/S1517-83822014005000003. 2014.

Han, Y., Han, L., Yao, Y., Li, Y., Liu, X., 2018. Key factors in FTIR spectroscopic analysis of DNA: the sampling technique, pretreatment temperature and sample concentration. Anal. Methods. 10 (21), 2436–2443. https://doi.org/10.1039/C8AY00386F.

Han, Y., Wang, X., Liu, Y., Han, L., Yang, Z., Liu, X., 2019. A novel FTIR discrimination based on genomic DNA for species-specific analysis of meat and bone meal. Food Chem. 294, 526–532. https://doi.org/10.1016/j.foodchem.2019.05.088.

Jangir, D.K., Tyagi, G., Mehrotra, R., Kundu, S., 2010. Carboplatin interaction with calf-thymus DNA: a FTIR spectroscopic approach. J. Mol. Struct. 969 (1–3), 126–129. https://doi.org/10.1016/j.molstruc.2010.01.052.

Joshi, B., Moreira, R.G., Omac, B., Castell-Perez, M.E., 2018. A process to decontaminate sliced fresh cucumber (Cucumis sativus) using electron beam irradiation. LWT 91, 95–101. https://doi.org/10.1016/j.lwt.2018.01.034.

Kanakis, C.D., Tarantilis, P.A., Polissiou, M.G., Diamantoglou, S., Tajmir-Riahi, H.A., 2005. DNA interaction with naturally occurring antioxidant flavonoids quercetin, kaempferol, and delphinidin. J. Biomol. Struct. Dyn. 22 (6), 719–724. https://doi.org/10.1080/07391102.2005.10507038.

Kneipp, J., Wittig, B., Bohr, H., Kneipp, K., 2010. Surface-enhanced Raman scattering: a new optical probe in molecular biophysics and biomedicine. Theor. Chem. Acc. 125 (3–6), 319–327. https://doi.org/10.1007/s00214-009-0665-2.

Kondepati, V.R., Keese, M., Heise, H.M., Backhaus, J., 2006. Detection of structural disorders in pancreatic tumour DNA with Fourier-transform infrared spectroscopy. Vib. Spectrosc. 40 (1), 33–39. https://doi.org/10.1016/j.vibspec.2005.06.003.

Kyung, H.K., Ramakrishnan, S.R., Kwon, J.H., 2019. Dose rates of electron beam and gamma ray irradiation affect microbial decontamination and quality changes in dried red pepper (Capsicum annuum L.) powder. J. Sci. Food Agric. 99 (2), 632–638. https://doi.org/10.1002/jsfa.9225.

Lee, M.H., Moon, Y.R., Chung, B.Y., Kim, J.S., Lee, K.S., Cho, J.Y., Kim, J.H., 2009. Practical use of chemical probes for reactive oxygen species produced in biological systems by γ-irradiation. Radiat. Phys. Chem. 78 (5), 323–327. https://doi.org/10.1016/j.radphyschem.2009.03.001.

Lee, S.L., Debenedetti, P.G., Errington, J.R., Pethica, B.A., Moore, D.J., 2004. A calorimetric and spectroscopic study of DNA at low hydration. J. Phys. Chem. B 108 (9), 3098–3106. https://doi.org/10.1021/jp0311409.

Letellier, R., Ghomi, M., Taillandier, E., 1989. Interpretation of DNA vibration modes: IV-a single-helical approach to assign the phosphate-backbone contribution to the vibrational spectra in A and B conformations. J. Biomol. Struct. Dyn. 6 (4), 755–768. https://doi.org/10.1080/07391102.1989.10507735.

Le-Tien, C., Lafortune, R., Shareck, F., Lacroix, M., 2007. DNA analysis of a radiotolerant bacterium Pantoea agglomerans by FT-IR spectroscopy. Talanta 71 (5), 1969–1975. https://doi.org/10.1016/j.talanta.2006.09.003.

Lindqvist, M., Gräslund, A., 2001. An FTIR and CD study of the structural effects of G-tract length and sequence context on DNA conformation in solution. J. Mol. Biol. 314 (3), 423–432. https://doi.org/10.1006/jmbi.2001.5164.

Lipiec, E., Kowalska, J., Lekki, J., Wiechec, A., Kwiatek, W.M., 2012. FTIR microspectroscopy in studies of DNA damage induced by proton microbeam in single PC-3

cells. Acta Phys. Pol. 121, 506–509. https://doi.org/10.12693/APhysPolA.121.506.
Liquier, J., Taillandier, E., 1996. Infrared spectroscopy of nucleic acids. In: Mantsch, H.H., Chapman, D. (Eds.), Infrared Spectroscopy of Biomolecules. Wiley-Liss, Inc, New York, pp. 131–158.
Li, S., Kundu, D., Holley, R.A., 2015. Use of lactic acid with electron beam irradiation for control of Escherichia coli O157: H7, non-O157 VTEC E. coli, and Salmonella serovars on fresh and frozen beef. Food Microbiol. 46, 34–39. https://doi.org/10.1016/j.fm.2014.06.018.
Malins, D.C., Hellström, K.E., Anderson, K.M., Johnson, P.M., Vinson, M.A., 2002. Antioxidant-induced changes in oxidized DNA. Proc. Natl. Acad. Sci. 99 (9), 5937–5941. https://doi.org/10.1073/pnas.082111199.
Miyahara, M., Saito, A., Ito, H., TOYODA, M., 2000. Capability for identification of gamma-irradiated bovine liver by new high sensitivity comet assay. Biol. Pharm. Bull. 23 (12), 1399–1405. https://doi.org/10.1248/bpb.23.1399.
Muntean, C.M., Lapusan, A., Mihaiu, L., Stefan, R., 2014. Strain dependent UV degradation of Escherichia coli DNA monitored by Fourier transform infrared spectroscopy. J. Photochem. Photobiol. B Biol. 130, 140–145. https://doi.org/10.1016/j.jphotobiol.2013.11.009.
Muntean, C.M., Stefan, R., Bindea, M., Cozma, V., 2013. Fourier transform infrared spectroscopy of DNA from Borrelia burgdorferi sensu lato and Ixodes ricinus ticks. Spectrochim. Acta A Mol. Biomol. Spectrosc. 110, 185–192. https://doi.org/10.1016/j.saa.2013.03.028.
Nikitaki, Z., Hellweg, C.E., Georgakilas, A.G., Ravanat, J.L., 2015. Stress-induced DNA damage biomarkers: applications and limitations. Front. chem. 3, 35. https://doi.org/10.3389/fchem.2015.00035.
Ovissipour, M., Rai, R., Nitin, N., 2019. DNA-based surrogate indicator for sanitation verification and predict inactivation of Escherichia coli O157: H7 using vibrational spectroscopy (FTIR). Food Control 100, 67–77. https://doi.org/10.1016/j.foodcont.2018.12.017.
Pouget, J.P., Frelon, S., Ravanat, J.L., Testard, I., Odin, F., Cadet, J., 2002. Formation of modified DNA bases in cells exposed either to gamma radiation or to high-LET particles. Radiat. Res. 157 (5), 589–595. https://doi.org/10.1667/0033-7587(2002)157[0589:FOMDBI]2.0.CO;2.
Roberts, P.B., 2016. Food irradiation: standards, regulations and world-wide trade. Radiat. Phys. Chem. 129, 30–34. https://doi.org/10.1016/j.radphyschem.2016.06.005.
Stefan, R., Muntean, C.M., Tripon, C., Halmagyi, A., Valimareanu, S., 2014. UV degradation of genomic DNA from in vitro grown plant species: a Fourier transform infrared spectroscopic assessment. Polym. Degrad. Stab. **108**, 35–40. https://doi.org/10.1016/j.polymdegradstab.2014.05.026.
Socrates, G., 2004. Infrared and Raman Characteristic Group Frequencies: Tables and Charts. John Wiley & Sons.
Taillandier, E., Liquier, J., 1992. [16] Infrared spectroscopy of DNA. Methods in Enzymology, vol. 211. Academic Press, pp. 307–335.
Taillandier, E., Liquier, J., 2002. Vibrational spectroscopy of nucleic acids. In: Chalmers, J.M., Griffiths, P.R. (Eds.), Handbook of Vibrational Spectroscopy Applications in Life, Pharmaceutical and Natural Sciences. John Wiley & Sons Ltd., Chichester, UK, pp. 3465–3480.
Thayer, D.W., Boyd, G., Fox Jr., J.B., Lakritz, L., Hampson, J.W., 1995. Variations in radiation sensitivity of foodborne pathogens associated with the suspending medium. J. Food Sci. 60, 63–67.
Tripon, C., Muntean, C.M., Surducan, E., Bratu, I., Halmagyi, A., Coste, A., 2016. Structural response of genomic DNA from grapevine (Vitis vinifera L.) varieties to microwaves irradiation: a Fourier transform infrared spectroscopy assessment. Biomed. Spectrosc. Imaging 5, 295–312.
Verbeek, F., Koppen, G., Schaeken, B., Verschaeve, L., 2008. Automated detection of irradiated food with the comet assay. Radiat. Prot. Dosim. 128 (4), 421–426. https://doi.org/10.1093/rpd/ncm433.
World Health Organization (WHO), 1999. High-dose Irradiation: Wholesomeness of Food Irradiated with Doses above 10 kGy. World Health Organization Technical Report Series. v890, Geneva, Switzerland Report of a joint FAO/IAEA/WHO study group.
Zanardi, E., Caligiani, A., Novelli, E., 2018. New insights to detect irradiated food: an overview. Food Anal. Methods. 11 (1), 224–235. https://doi.org/10.1007/s12161-017-0992-1.
Zhang, Y., Zhang, G., Fu, P., Ma, Y., Zhou, J., 2012. Study on the interaction of triadimenol with calf thymus DNA by multispectroscopic methods and molecular modeling. Spectrochim. Acta A Mol. Biomol. Spectrosc. 96, 1012–1019. https://doi.org/10.1016/j.saa.2012.08.002.
Zhou-Sun, B.W., Liquier, J., Taillandier, E., Sun, J.S., Garestier, T., Hélène, C., Gryaznov, S.M., 1997. A physico-chemical study of triple helix formation by an oligodeoxythymidylate with N3′→ P5′ phosphoramidate linkages. Nucleic Acids Res. 25 (9), 1782–1787. https://doi.org/10.1093/nar/25.9.1782.